Conference on MODELLING FLUID FLOW (CMFF'12)

September 4-7, 2012

Budapest University of Technology and Economics
Budapest, Hungary

THE 15th EVENT OF INTERNATIONAL CONFERENCE SERIES
ON FLUID FLOW TECHNOLOGIES HELD IN BUDAPEST

CONFERENCE PROCEEDINGS

Volume I.

Edited by
J. Vad
Department of Fluid Mechanics
Budapest University of Technology and Economics

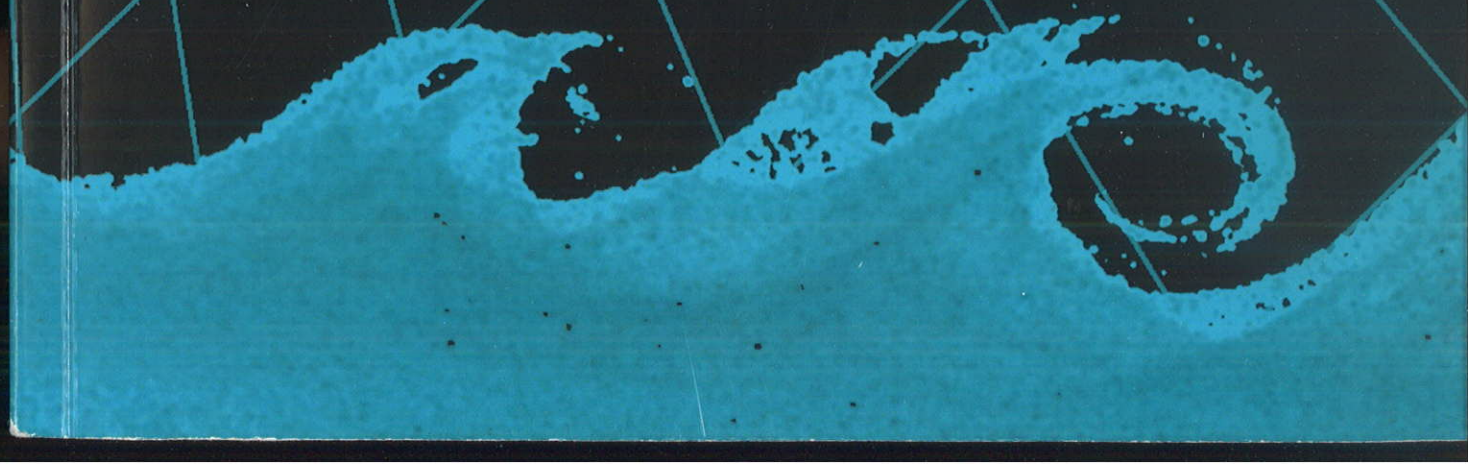

Conference on Modelling Fluid Flow (CMFF'12)
The 15th International Conference on Fluid Flow Technologies
Budapest, Hungary, September 4-7, 2012

HEAT TRANSFER AND INTERNAL WAVES IN A RECIPROCATING COMPRESSOR

Thomas Müllner[1], Herbert Steinrück[2]

[1]Vienna University of Technology, Institute of Fluid Mechanics and Heat Transfer, Resselgasse 3, 1040 Vienna, Austria, E-mail: thomas.muellner@tuwien.ac.at
[2]Corresponding author. Vienna University of Technology, Institute of Fluid Mechanics and Heat Transfer, Resselgasse 3, 1040 Vienna, Austria, Tel.: +43 1 58801 32231, Fax +43 1 58801 32299, E-mail: herbert.steinrueck@tuwien.ac.at

ABSTRACT

The internal flow in a reciprocating compressor, its interaction with the valves, and the heat transfer from the compressed gas to the compressor housing are studied using different flow and heat transfer models. For simple compressors, having only one suction and one discharge valve it turns out that a one dimensional non-linear flow model is sufficient to describe the interaction of the internal pressure waves with the valves. For more complex geometries 2D- or 3D-flow models are required.

Although a one dimensional model seems insufficient to predict the heat transfer in the compressor, which depends on the internal flow structure, a method has been developed, how a reasonable approximation of the heat fluxes can be obtained by expressing the heat-fluxes as a weighted sum of four reference enthalpy fluxes resulting from the 1D-flow model. The weight factors can be interpreted as Stanton numbers and have to be determined a priory by 3D-CFD simulations. The gain of this approach is that these Stanton numbers have to be determined only once for a certain class of compressors and depend only weakly on the compressor data.

Keywords: reciprocating compressor, internal waves, heat transfer

NOMENCLATURE

A	area
$\dot{Q}$	heat flow
Z	distance cylinder head piston
St	Stanton number
c	speed of sound
c_p	specific isobaric heat capacity
c_v	specific isochoric heat capacity
d	diameter
e	specific internal energy
f	compressor speed
h	stroke
k_S	valve spring constant
$\dot{m}$	mass flow
m_V	mass valve plate
p	pressure
$\dot{q}$	heat flux density
s	specific entropy
t	time
u	gas velocity
$\underline{u}$	state vector
x	coordinate along diameter
y	coordinate perpendicular to diameter
z	coordinate in axial direction
z_V	valve lift
γ	ratio of specific heat capacities
φ	crank angle
λ	shock speed
ρ	gas density

1. INTRODUCTION

The cross section of a reciprocating compressor is shown in Figure 1. It consists of a cylindrical compression chamber closed at one end by the cylinder head and at the other end by a movable piston. During the expansion phase the volume in the compression chamber increases, and gas enters through the suction valve. After the piston has reached the position of maximal volume, it starts to compress the gas. If the pressure in the compression chamber exceeds the discharge pressure, the discharge valve opens, and the gas leaves the compressor through the discharge valves.

Until recently for the design of a compressor a quasi static description of the gas in the compressor has been sufficient [2]. However, due to the design of larger and faster compressors it turns out that internal waves cannot be neglected. They result in unwanted valve losses or in large oscillating moments on the piston rod [3].

The suction and discharge valves are usually

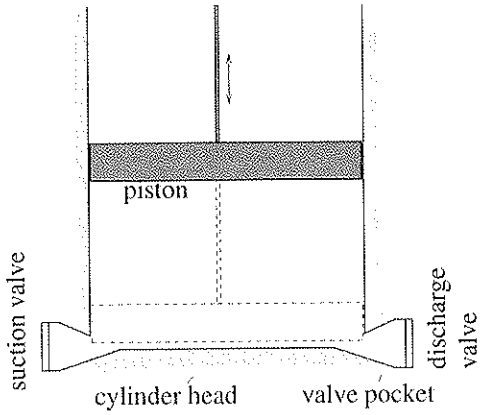

Figure 1: Reciprocating compressor

situated at the cylinder barrel near the cylinder head. They are connected to the cylinder by valve pockets (see Figure 1). The valves are passive. That means a valve opens if there is a sufficient positive pressure difference across it; otherwise it is closed. If the discharge valve opens, a rarefaction wave is initiated. It is reflected at the opposite side of the cylinder and thus interacts with the discharge valve. As a consequence, the discharge valve may open and close several times during discharge.

For the design of a compressor, the interaction of the internal waves with the valves is essential since the waves contribute to losses of efficiency.

A series of models has been developed (1D-, 2D-, and 3D) to describe the interaction of the valves with the internal waves and the fluid flow based on the Euler equations.

In the 1D-case the wave propagation between the suction and discharge valve is modeled by the quasi 1D-Euler equations, see Aigner [1]. Although, this model is very simple, reasonable qualitative agreement with experiments have been obtained. However, for compressors with more than one suction or discharge valve at least a 2D-flow model is necessary. A comparison of the wave propagation models (1D, 2D, 3D) and with experiments will be given.

For the design of a compressor the heat transfer of the gas to the surrounding compressor walls is also of interest. For internal combustion engines a relation for the instantaneous heat transfer coefficient was given by Woschni [6].

For the heat transfer analysis a 3D-flow simulation seems to be necessary. However, we have developed an approach to estimate the heat transfer by using the the 1D-flow model. The main idea is that the heat transfer is proportional to a weighted sum of enthalpy fluxes which can be determined by the 1D-flow model. The weights can be interpreted as Stanton numbers. Thus empirical relations for these Stanton numbers are needed. They can be obtained a priori on a data base generated by 3D-flow simulations.

Thus, a fast, reliable tool for the compressor design has been developed which is capable predicting internal waves, impact speed of the valve plate onto the valve seat and heat transfer.

The paper is organized as follows. In section 2 we review flow models, and compare their predictions with measurements. In section 3 we present a heat transfer model.

2. Flow models

Since, under normal operating conditions, the Reynolds number is very large, the flow field of the gas in the compressor is turbulent, and thus, the Reynolds Averaged Navier Stokes (RANS) equations can be used to describe the flow field. However, solving the RANS equations with a commercial code in a 3D domain is very much time consuming. Thus, there is a need for simplified flow models which will be described in the following.

2.1. 1D-Flow model

Let us consider a simple compressor with just one suction and one discharge valve sitting opposite to each other at the circumference of the compression chamber first. The following two observations justify a one dimensional approach:

- Internal waves are initiated when the discharge valves opens. Then the piston is sufficient close to the cylinder head, and the flow takes place in a narrow gap between the cylinder head and the piston.
- Waves travel mainly back and forth between the discharge and suction valve.

When the piston is not close to the cylinder head, the flow is three dimensional. However, usually during this stage waves have been already damped.

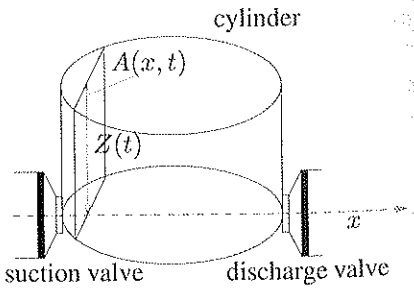

Figure 2: Cross section in 1D-flow model

Let x denote the spatial coordinate along the diameter between the valves. The state of the gas at a position x and time t is denoted by $\underline{u} = (\rho, \rho u, \rho e + \rho u^2/2)$, where u is the flow velocity in x-direction, ρ the density of the gas and e the specific inner energy. Furthermore, let $A(x,t)$ be the cross section of the compressor perpendicular to the x-axis, see Figure 2. It is of course a function of x and t. Assuming that all

flow quantities are functions of x and t, the mass- and momentum balance read:

$$(A\rho)_t + (A\rho u)_x = 0, \tag{1}$$

$$(A\rho u)_t + (A\rho u^2 + Ap)_x = pA_x. \tag{2}$$

$$\left(A\rho(e + \frac{u^2}{2})\right)_t + \left(A\rho u(e + \frac{p}{\rho} + \frac{u^2}{2})\right)_x = -A_t p, \tag{3}$$

where p is the pressure and $e = e(p, \rho)$ is the specific internal energy given by equation of state.

Instead of using the energy equation in [1] it is assumed that the flow is isentropic and smooth (no shocks). Thus (2) is replaced by

$$\rho_t + \left(\frac{u^2}{2} + \int_{\rho_0}^{\rho} \frac{c^2(\tilde{\rho}, s_0)}{\tilde{\rho}} \mathrm{d}\tilde{\rho}\right)_x = 0, \tag{4}$$

where c is the isentropic speed of sound, and s is the specific entropy.

2.1.1. Discontinuous cross section

At the connection of the valve pocket to the compression chamber the cross section A has a discontinuity. Thus, the 1D-flow model is there of limited accuracy since the flow is there locally three dimensional. However, we want to model this discontinuity in the frame work of a one dimensional Euler flow.

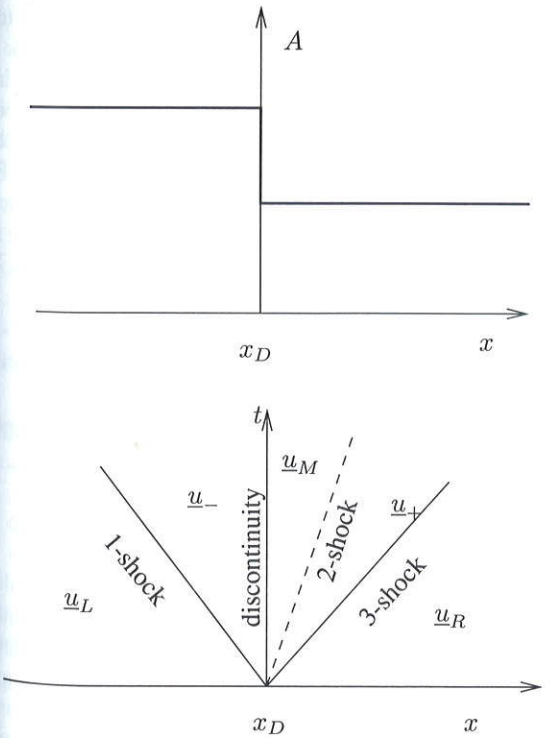

Figure 3: Riemann problem with discontinuity of cross section

Using a finite volume scheme for the discretization of the flow equation, we place the control volume such that there is a cell boundary at the discontinuity located at x_D. The basic idea is now to determine the numerical flux at both sides of this cell boundary. Since, the cross section A is discontinuous there, the flux is there also discontinuous. However, the mass and enthalpy fluxes are continuous. Only the momentum flux and the pressure are discontinuous. Now following the basic idea of Gudunov's method [5], we solve a Riemann problem where the initial data is discontinuous at the cell boundary. The solution structure for subsonic flow from left to right is depicted in Figure 3. The x,t-half-plane is divided by shocks, expansion fans or the discontinuity of the cross section into four regions, see Figure 3.

Across a shock the Rankine-Hugoniot conditions hold. For example for the 1-shock we have:

$$\rho_L u_L - \rho_- u_- = \lambda_1(\rho_L - \rho_-), \tag{5}$$

$$\rho_L u_L^2 + p_L - \rho_- u_-^2 - p_- = \lambda_1(\rho_L u_L - \rho_- u_-), \tag{6}$$

$$\begin{aligned}\rho_L u_L(h_L + \tfrac{u_L^2}{2}) - \rho_- u_-(h_- + \tfrac{u_-^2}{2}) = \\ \lambda_1(\rho_L(e_L + \tfrac{u_L^2}{2}) - \rho_-(e_- + \tfrac{u_-^2}{2}))\end{aligned}, \tag{7}$$

where λ_1 is the speed of the 1-shock and $\underline{u}_L$ is the state vector left of the 1-shock and $\underline{U}_-$ is the vector right of the 1-shock. For the 3-shock the same conditions hold for the state vectors $\underline{u}_+$ and $\underline{u}_R$ left and right of the 3-shock and the shock speed λ_3. Across a 2-shock the pressure and flow velocity are continuous.

To obtain a relation between $\underline{u}_-$ and $\underline{u}_M$ we assume a stationary isentropic flow in case of a decrease of the flow cross section in flow direction. In case of a sudden increase of the cross section, we use the Borda-Carnot pressure loss.

In both cases a non-linear equation for the flow velocity u_- can be derived which has to be solved iteratively. Thus, the states $\underline{u}_-$ and $\underline{u}_M$ can be determined and the mass, momentum, and energy flow and the pressure on both sides of the discontinuity can be obtained and prescribed in the finite volume scheme.

Note that we have discussed only the simplest case of subsonic flow with $u_- > 0$. Depending on the sign of the shock speeds we have to distinguish several cases similar to Gudunov's method. However, here an additional case can occur, when in the $-$-region the flow is subsonic, but reaches critical flow conditions $\underline{u}_C$ after the restriction of the cross section at $x = x_D+$. In this case an expansion fan to supersonic flow follows, see Figure 4.

2.2. 2D-Flow model

Since, the waves are mainly initiated by the opening and closing of the discharge valves, wave phenomena are of primary interest, only when the distance between the piston and cylinder head is small compared to the diameter of the cylinder. Thus, during discharge the flow can be approximated by a 2D-dimensional flow parallel to the cylinder head.

Let $Z = Z_p(t) - z_H(x, y)$ be the distance between the cylinder head and the piston, where $Z_p(t)$ denotes

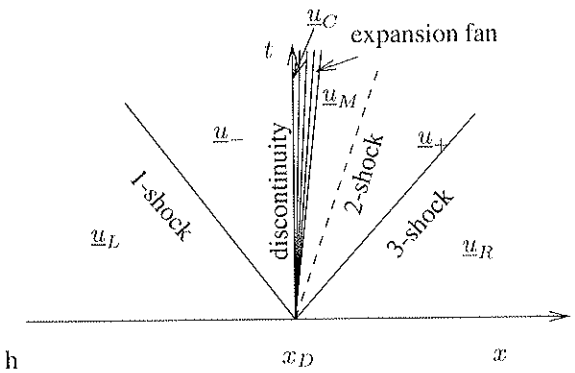

Figure 4: Riemann problem with critical flow conditions downstream of the discontinuity of the cross section

the actual position of the piston at time t and $z = z_H(x, y)$ is the surface of the cylinder head.

Assuming isotropic flow the governing equations are:

$$(\rho Z)_t + (\rho Z u)_x + (\rho Z v)_y = 0, \quad (8)$$

$$(\rho Z u)_t + (\rho Z u^2 + pZ)_x + (\rho Z u v)_y = pZ_x, \quad (9)$$

$$(\rho Z v)_t + (\rho Z u v)_x + (\rho Z v^2 + pZ)_y = pZ_y, \quad (10)$$

where ρ, u, v are the density and the velocity components in x and y direction, respectively. The pressure is given by the equation of state $p = p(\rho, s)$.

2.3. Valve model

2.3.1. Mass flow

In Figure 5 a plate valve is sketched. The valve plate is pressed to the valve seat by springs and by the pressure p_2 behind the valve acting on the effective area A_V. If the pressure p_1 in front of the valve exceeds the pressure p_2 and the spring force, the valve begins to open. The position z_V of the valve plate is governed by the equation of motion

$$m_V \ddot{z}_V = (p_1 - p_2)A_V - k_s(z_V + l_1), \quad (11)$$

where m_V is the mass of the valve plate, k_s the spring constant and, l_1 an initial deflection. The valve lift z_V is limited by 0 (closed valve) and the maximum valve lift $z_{V,\max}$ (valve completely open).

The mass flow through the valve is given by:

$$\dot{m} = \phi \rho_1 \left(\frac{p_2}{p_{t1}}\right)^{1/\gamma} \sqrt{\frac{2\gamma}{\gamma - 1}\frac{p_{t1}}{\rho_1}\left(1 - \left(\frac{p_2}{p_{t1}}\right)^{\frac{\gamma-1}{\gamma}}\right)}, \quad (12)$$

where p_{t1} is the total pressure in front of the valve and $\phi = \phi(z_V)$ is the effective flow cross section which is a function of the valve lift z_V only [2] .

2.3.2. Implementing the boundary condition

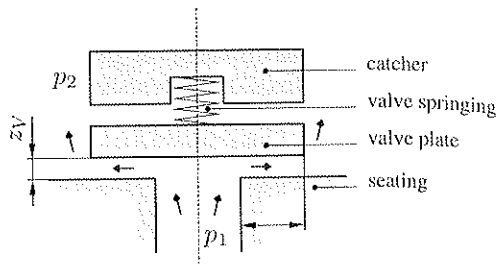

Figure 5: Scheme of a passive plate valve

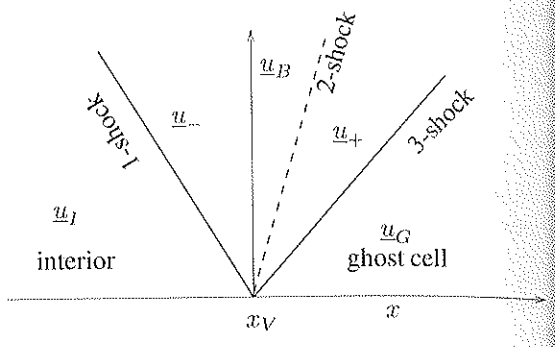

Figure 6: Prescribing boundary conditions

In order to prescribe the mass flow given by eq. (12) at the boundary of the computational domain $x = x_V$, we proceed as follows:

Inspired by Gudonov's method, we first extend the computational domain to a ghost cell adjacent to the boundary. Let $\underline{u}_I$ denote the state vector in the first interior cell, and and assume the state vector $\underline{u}_G$ in the ghost cell is known. Now solving the Riemann problem for the first interior cell and the ghost cell, we obtain the state values $\underline{u}_B$ at the boundary, and thus, the Euler flux $\underline{F}(\underline{u}_B)$. The solution of the Riemann problem is given by three shocks or expansion fans radiating from the discontinuity at the boundary with the speeds $\lambda_1 < \lambda_2 < \lambda_3$.

Let $\underline{u}_-$ and $\underline{u}_+$ the states between the 1- and 2-shock and between the 2- and 3- shock, respectively (see Figure 6).

In case of a 1-shock, the Rankine-Hugoniot conditions (5)-(7) hold by replacing $\underline{u}_L$ and $\underline{u}_-$ with $\underline{u}_I$ and $\underline{u}_-$.

Across the 2-shock the pressure and the flow velocity are constant $u_- = u_+$ and $p_- = p_+$. In case of outflow $\dot{m} > 0$, the boundary value is $\mathbf{u}_B = \mathbf{u}_-$. Thus, the Rankine-Hugoniot conditions are supplemented with the condition for the mass flow. In case of inflow $\dot{m} < 0$ the boundary value is $\underline{u}_B = \underline{u}_+$. Additionally to the mass flow a second boundary condition can be prescribed, e. g. the entropy of the gas $s_+ = s_B$ entering the compressor. Let $\rho(s, p)$ denote the density as a function of the entropy and pressure. Using that the pressure and the flow velocity are constant across the 2-shock the following conditions to supplement the quasi 1D-Euler equations (1)-(3) are obtained.

$$\dot{m} = \begin{cases} A\rho_- u_-, & \dot{m} > 0, \\ A\rho(s_B, p_-)u_-, & \dot{m} < 0. \end{cases} \qquad (13)$$

An alternative way to implement the boundary condition is, to prescribe the total pressure $p_{t,G}$ and the entropy s_G in the ghost cell, and to determine the flow velocity in the ghost cell such, that when applying a finite volume scheme to the interior cell I and the ghost cell G, the numerical flux at the boundary yields the prescribed mass flow. A similar approach was used by [1]. The advantage of this method is that is can be applied to all finite volume schemes while the first method is essentially Gudonov's scheme, which is of first order.

2.4. Results

In order to evaluate the different flow models, a compressor with the main specifications given in table 1 has been chosen. For details, see [4]. The compressor has one suction and one discharge valve. Thus, the 1D-model can be applied (see figure 7). The pressure at the locations, shown in Fig. 4, has been measured at the test compressor and compared to the predictions given by the different numerical models.

Table 1: Specifications of the test compressor

diameter	d_p	0.2 m
stroke	h	90 mm
speed	f	16.3 1/s
suction press.	p_{suc}	1 bar
discharge press.	p_{dis}	5 bar
inlet Temp.	T_{in}	300 K
medium		air

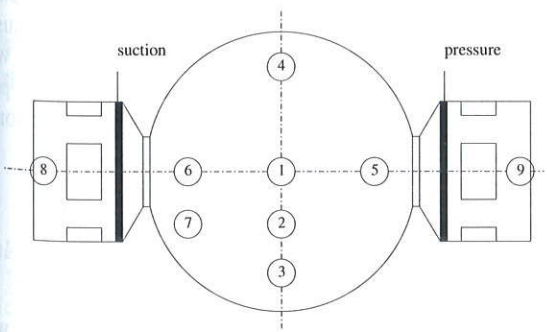

Figure 7: Location of pressure sensors in the cylinder

In Figure 8, the pressure difference between the sensors pc6 and pc5 computed with the 1D-, 2D-and 3D-flow model is shown. For the 1D-model 330 cell per diameter have been used, for the 2D-model 104 cells, and for the 3D-model (FLUENT) 70 cells per diameter. The computation time for two revolutions had been 2 minutes, 4 hours, and 2.5 days for the 1D-, 2D-, and 3D-simulation program, respectively.

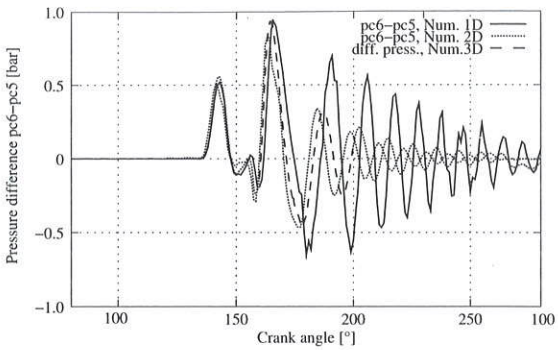

Figure 8: Internal pressure waves: comparison of different flow models for the pressure difference between suction and discharge side in the cylinder

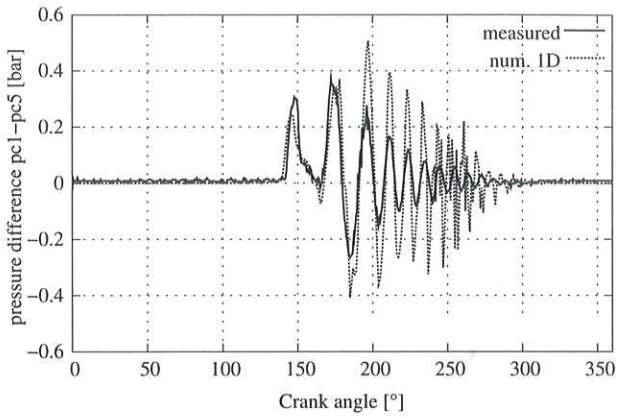

Figure 9: Internal pressure waves: comparison measurement and 1D-flow model for the pressure difference between suction side and center

The difference of the pressures at the positions pc6 and pc5 is an indicator of internal waves. The first peak in the pressure difference corresponds to the rarefaction wave due to the opening of the discharge valve at a crank angle of about 135°. The predictions of all three models agree up to a crank angle of about 160°, and differ only slightly up to 180°. The discharge valve closes, shortly after the piston has reached the dead point at a crank angle of 180°. During the beginning expansion phase, internal waves remain in the compression chamber. However, the results for the 2D-, and 3D-flow model agree reasonably well. The damping of the waves predicted by the 1D-model is much weaker.

In Figure 9, a comparison of the predictions of the 1D-model with measured data is given. There is a good agreement during the discharge phase. During expansion, waves, traveling back and forth, can be observed. Again, the damping of the waves, predicted by the 1D-model, is weaker than damping of the measured pressure waves. The damping rate of the predictions of the 2D- and 3D-model are approximately the same as the damping rate of the measured data. All signals have the same frequency which can be estimated by the speed of sound and the distance

between the two valves.

3. Heat Transfer

3.1. Heat transfer modeling

A disadvantage of the simple 1D-model is that it is not capable to calculate the heat transfer. Thus another strategy is adopted. The basic idea is to relate the wall heat flux density to a reference enthalpy flux density

$$\dot{q} = St \cdot \dot{h}_{\mathrm{ref}} = St \cdot c_p \Delta T_{\mathrm{ref}} \rho_{\mathrm{ref}} u_{\mathrm{ref}}, \qquad (14)$$

where St is a suitable Stanton number, and ΔT_{ref}, ρ_{ref}, u_{ref} are suitable reference values for the temperature difference, the gas density, and the flow velocity, respectively. The cycle of a compressor consists of four phases: inflow, compression, discharge, expansion.

3.1.1. Inflow

The gas enters through the suction valve. Thus a jet of cold gas emanating at the suction valve and impinges onto the piston rod or surfaces adjacent to the suction valve. The reference velocity from the inlet mass flow $\dot{m}_{\mathrm{in}}$ through the suction valve is given by:

$$u_{\mathrm{ref,in}} = \dot{m}_{\mathrm{in}} / \left(\rho_{\mathrm{in}} A_{\mathrm{cross}}(t)\right), \qquad (15)$$

where the $A_{\mathrm{cross}}(t) = d_p\, Z(t)$ is the cross section of the compression chamber along the piston rod and $Z(t)$ is the distance of the piston from the cylinder head. The reference density ρ_{ref} is taken from the values of the thermodynamic state of the gas at inflow, $\rho_{\mathrm{ref}} = \rho_{\mathrm{in}}$.

The heat transfer will be influenced after some retardation time t_0, since it takes some time for the cold gas to impinge at the surfaces of the compression chamber. Thus the associated heat flux through a surface of area $A(t)$ of the compression chamber is written as a function of the time t as:

$$\dot{Q}_{\mathrm{in}}(t) = St_{\mathrm{in}} c_p (T_w - T_{\mathrm{in}}) \frac{A(t)}{A_{\mathrm{cross}}(t)} \dot{m}_{\mathrm{in}} (t - t_0). \qquad (16)$$

The retardation time t_0, defined as the time the inflow jet with velocity u_{injet} needs to reach the center of the cylinder, is given by

$$t_0 = \frac{d}{2u_{\mathrm{injet}}}. \qquad (17)$$

The inflow velocity u_{injet} is estimated by

$$u_{\mathrm{injet}} = \frac{\dot{m}_{\mathrm{in}}}{\rho A_{\mathrm{eff}}}, \qquad (18)$$

where A_{eff} is the effective flow cross section of the inflow path. We approximate A_{eff} by the cross section A_{slot} of the opening between the cylinder and the valve pocket times an empirical factor f_{ret}, $A_{\mathrm{eff}} = A_{\mathrm{slot}} f_{\mathrm{ret}}$. We choose

$$f_{\mathrm{ret}} = \begin{cases} 2.5 & \text{piston, head, piston rod} \\ 5.0 & \text{cylinder barrel} \end{cases}. \qquad (19)$$

The main surfaces of the compression chamber are the piston, cylinder cap, piston rod and the cylinder barrel. Their areas are

$$\begin{aligned} A_{\mathrm{rod}} &= \pi d_{\mathrm{rod}} Z(t), \\ A_{\mathrm{pist}} &= A_{\mathrm{head}} = \pi d_p^2/4, \\ A_{\mathrm{side}} &= \pi d_p Z(t). \end{aligned} \qquad (20)$$

3.1.2. Outflow

During outflow, it is expected that the flow is dominated by the outflow of the gas. Similar to the inflow phase, the reference velocity

$$u_{\mathrm{ref,out}} = \dot{m}_{\mathrm{out}} / \left(\rho_{\mathrm{out}} A_{\mathrm{cross}}(t)\right) \qquad (21)$$

is used. The choice of a reference density is not of relevance since it does not appear in the formula for the heat flux density when expressing the heat flux density in terms of the mass flow.

Thus the local velocities will be proportional to the out going mass flow $|\dot{m}_{\mathrm{out}}|$. Thus the heat transfer related to the out going mass flow is

$$\dot{Q}_{\mathrm{out}}(t) = St_{\mathrm{out}} c_p \frac{A(t)}{A_{\mathrm{cross}}(t)} \dot{m}_{\mathrm{out}} (T_w - T_{\mathrm{gas}}). \qquad (22)$$

For the outflow phase, no retardation time is necessary since the information, that the valve is open, spreads with the speed of sound which is considerable larger than the actual flow velocity.

3.1.3. Compression and Expansion

In the compression phase a natural reference velocity is the actual velocity of the piston $u_p(t)$. However, at the turning points of the piston motion, it is zero, but the heat flux density will not vanish. Thus as a second reference velocity is chosen, $u_m = h \cdot f$, which is $\frac{2}{\pi}$ times the average of the modulus of the piston speed. Thus, the heat transfer during compression and expansion is given by

$$\dot{Q}_{\mathrm{comp}} = \left(St_p \frac{u_p(t)}{u_m} + St_m \right) \rho_{\mathrm{isen}} u_m c_p \Delta T A(t). \qquad (23)$$

As reference density, the density ρ_{isen}, which results from an isentropic change of state from the inflow condition $(\rho_{\mathrm{in}}, T_{\mathrm{in}})$ to the actual gas temperature T in the compressor, is used.

Assume a constant isochoric heat capacity c_v of the ideal gas. Then the density ρ_{isen} is given by

$$\rho_{\mathrm{isen}}(T) = \rho_{\mathrm{in}} \left(\frac{T}{T_{\mathrm{in}}} \right)^{\frac{1}{\gamma - 1}} \qquad (24)$$

Summarizing the reconstructed heat flux $\dot{Q}_{\mathrm{rec}}(t)$ has the form

$$\dot{Q}_{\mathrm{rec}}(t) =$$

$$\left(St_{\mathrm{in}} \frac{\dot{m}_{\mathrm{in}}(t-t_0)}{A_{\mathrm{cross}}(t)} + St_{\mathrm{out}} \frac{\dot{m}_{\mathrm{out}}}{A_{\mathrm{cross}}(t)} \right. \tag{25}$$

$$\left. + St_p u_p(t) \rho_{\mathrm{isen}} + St_m \rho_{\mathrm{isen}} u_m \right)$$

$$\cdot A(t) \bar{c}_p (T_w - T_{\mathrm{gas}}).$$

3.2. Results

First a commercial CFD program, FLUENT, is used to calculate the heat fluxes $\dot{Q}_{\mathrm{num}}$ through the faces of the compression chamber (piston, cylinder head, barrel, piston rod). Additionally to the compressor data given in Table 1 and the properties of the gas (air), the wall temperature $T_w = 400\,\mathrm{K}$ has been prescribed. The heat fluxes $\dot{Q}_{\mathrm{num}}$ calculated by FLUENT through the side wall and the cylinder head are shown in Figures 10 and 11 by the solid line as a function of the crank angle, respectively. Note, that the area of the side wall $A_{\mathrm{side}}(t)$ changes with time due to the piston motion, while A_{head} is constant.

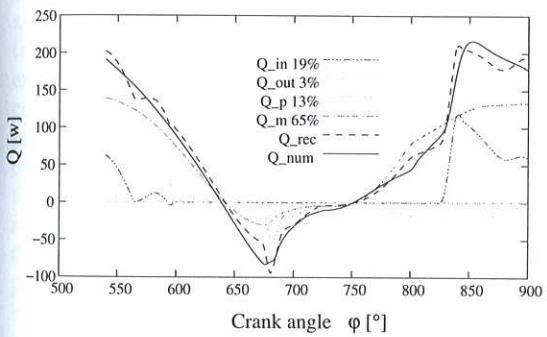

Figure 10: Components of the reconstructed heat flux through the side wall

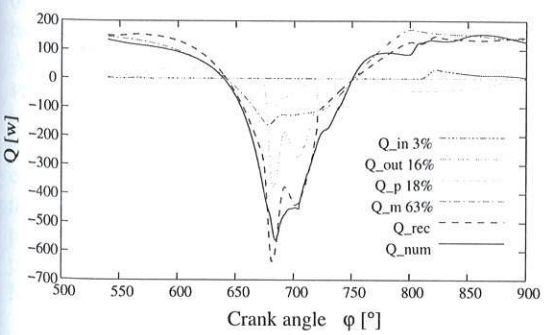

Figure 11: Components of the reconstructed heat flux through the cylinder head

At a crank angle angle of 540°, the compression chamber has its maximal volume. The gas temperature is almost equal to the inlet temperature of $T_{\mathrm{in}} = 300\,\mathrm{K}$. Thus, the heat flow is directed into the compression chamber (positive sign). Then the compression starts, the temperature of the gas rises, and the heat flux decreases. At a crank angle of about 640°, the gas temperature is equal to the wall temperature, and the direction of the heat flow is reversed.

At a crank angle of 680°, the discharge valve opens, and the flow is dominated by the outflow which is strongly influenced by the valve motion. However, this valve motion causes rapid variations in the heat flux.

During expansion, the gas temperature decreases. In this stage, the heat flux is again dominated by the flow induced by the piston motion until the suction valves opens at about 830°, resulting in a sharp increase of the heat flux through the side walls.

In order to reconstruct the heat fluxes from data available from a 1D-flow model, the Stanton numbers have to be known. They are determined such, that the reconstructed heat flux $\dot{Q}_{\mathrm{rec}}$ approximates the heat flux $\dot{Q}_{\mathrm{num}}$ determined by the CFD code best in the sense of least squares. The quadratic approximation error

$$\int_0^{t_p} (\dot{Q}_{\mathrm{num}}(t) - \dot{Q}_{\mathrm{rec}}(t))^2 \mathrm{d}t \to \min \tag{26}$$

over a complete compression cycle with period t_p has to be minimized. The results for the Stanton numbers for the cylinder head and the side wall are listed in Table 2.

Table 2: Stanton numbers

	head	side wall
St_{in}	$1.01 \cdot 10^{-3}$	$4.3 \cdot 10^{-3}$
St_{out}	$-0.74 \cdot 10^{-3}$	$-0.47 \cdot 10^{-3}$
St_{p}	$-4.9 \cdot 10^{-3}$	$-3.1 \cdot 10^{-3}$
St_{m}	$51.8 \cdot 10^{-3}$	$-36.3 \cdot 10^{-3}$
rel. error	18%	10 %

The Stanton number St_{out} is negative since the out going mass flow $\dot{m}_{\mathrm{out}}$ is negative. The Stanton number St_p is a correction to the mean piston velocity, and thus, its sign has no direct physical interpretation.

The reconstructed heat flux for both faces is shown in the figures 10 and 11, respectively. The relative error is about 18% for the cylinder head and 10% for the side walls. The approximation of the heat flux through the side wall is better since the area of the side wall during the outflow is smaller. Additionally the contributions of the four components to the reconstructed heat flux are also indicated. Obviously the main component is associated with the heat flux due to the piston motion (about 80%). The heat flux associated with the outflow has a significant influence on the heat flux through the cylinder head but is negligible for the side wall. The heat flux associated with the inflow has a significant contribution to the heat flux through the side wall but almost no influence on the heat flux through the cylinder head.

4. CONCLUSIONS

Flow models have been discussed to predict internal waves and a heat transfer analysis of a reciprocating compressor. Although these quantities can be predicted by commercial codes, there is a need for fast easy to handle models using only a fraction of the computational effort. For internal waves, it has been shown, that, in case of a simple compressor, a 1D-flow model is sufficient. For the heat transfer analysis a 1D-flow model is also sufficient provided that a data base for dimensionless coefficients, Stanton numbers, for compressors under similar operation conditions is available.

ACKNOWLEDGMENTS

This work was funded by the EFRC, European Forum of Reciprocating Compressors.

REFERENCES

[1] Aigner, R., (2007), "Internal Flow and Valve Dynamics in a Reciprocating compressor", PhD-thesis TU Vienna, Institute of Fluid Mechanics and Heat Transfer.

[2] Costagliola, M, (1950), "The theory of spring loaded valves for reciprocating compressors", J. Appl. Mech. pp. 415-420.

[3] Machu, E., (1998), "Problems with high speed short stroke compression: Increased power requirements due to pocket losses, piston masking and gas inertia, eccentric loads on piston", Proc. of Gas Machinery Conference, USA.

[4] Steinrück, H., Aigner, R., and Machu, G., (2008), "Transversal waves in a reciprocating compressor", Acta Mech., Vol. 201, pp. 231-248.

[5] Toro, E., (1999), *Riemann solvers and Numerical methods for Fluid Dynamics*, Springer.

[6] Woschni, G., (1967), "A Universal Applicable Equation for the Instantaneous Heat Transfer Coefficient in the Internal Combustion Engine", SAE technical paper 670931.